HHS Public Access

Author manuscript

J Leukoc Biol. Author manuscript; available in PMC 2020 December 08.

Published in final edited form as:

J Leukoc Biol. 2020 June ; 107(6): 1069–1079. doi:10.1002/JLB.5MA0120-228R.

TEG011 persistence averts extramedullary tumor growth without exerting off-target toxicity against healthy tissues in a humanized HLA-A*24:02 transgenic mice

Inez Johanna[1], **Patricia Hernández-López**[1], **Sabine Heijhuurs**[1], **Laura Bongiovanni**[2], **Alain de Bruin**[2], **Dennis Beringer**[1], **Sanne van Dooremalen**[1], **Leonard D. Shultz**[3], **Fumihiko Ishikawa**[4], **Zsolt Sebestyen**[1], **Trudy Straetemans**[1], **Jürgen Kuball**[1]

[1]Department of Hematology and Center for Translational Immunology, University Medical Center Utrecht, Utrecht, The Netherlands [2]Department of Pathobiology, Dutch Molecular Pathology Center, Faculty of Veterinary Medicine, Utrecht University, Utrecht, The Netherlands [3]Department of Immunology, The Jackson Laboratory, Bar Harbor, Maine, USA [4]Laboratory for Human Disease Models, RIKEN Center for Integrative Medical Sciences, Yokohama, Japan

Abstract

$\gamma\delta$T cells play an important role in cancer immunosurveillance and are able to distinguish malignant cells from their healthy counterparts via their $\gamma\delta$TCR. This characteristic makes $\gamma\delta$T cells an attractive candidate for therapeutic application in cancer immunotherapy. Previously, we have identified a novel CD8α-dependent tumor-specific allo-HLA-A*24:02-restricted Vγ5Vδ1TCR with potential therapeutic value when used to engineer $\alpha\beta$T cells from HLA-A*24:02 harboring individuals. $\alpha\beta$T cells engineered to express this defined Vγ5Vδ1TCR (TEG011) have been suggested to recognize spatial changes in HLA-A*24:02 present selectively on tumor cells but not their healthy counterparts. However, in vivo efficacy and toxicity studies of TEG011 are still limited. Therefore, we extend the efficacy and toxicity studies as well as the dynamics of TEG011 in vivo in a humanized HLA-A*24:02 transgenic NSG (NSG-A24:02) mouse model to allow the preparation of a first-in-men clinical safety package for adoptive transfer of TEG011. Mice treated with TEG011 did not exhibit any graft-versus-host disease-like symptoms and extensive analysis of pathologic changes in NSG-A24:02 mice did not show any off-target toxicity of TEG011. However, loss of persistence of TEG011 in tumor-bearing mice was associated with the outgrowth of extramedullary tumor masses as also observed for mock-treated

Correspondence Jürgen Kuball, University Medical Center, Utrecht, Heidelberglaan 100, 3584 CX Utrecht, The Netherlands. J.H.E.Kuball@umcutrecht.nl.

AUTHORSHIP

I.J., T.S., Z.S., and J.K. conceptualized, designed, and developed the in vivo models. I.J., P.H.-L., and S.H. performed the in vivo experiments. L.B. and A.B. performed the histopathology and IF examination of the mouse tissues. D.B., L.D.S., and F.I. contributed vital components. I.J., J.K., and S.vD. conceptualized, designed, and made the graphical abstract. I.J. analyzed all in vivo data and was a major contributor in writing the manuscript. I.J., T.S., Z.S., and J.K. interpreted all in vivo data. I.J. and J.K. wrote the manuscript; and all authors read, reviewed, and approved the final manuscript.

DISCLOSURES

D.B., Z.S., and J.K. are inventors on different patents with $\gamma\delta$TCR sequences, recognition mechanisms, and isolation strategies. J.K. is scientific advisor and shareholder of Gadeta (www.gadeta.nl). No potential conflicts of interest were disclosed by the other authors.

SUPPORTING INFORMATION

Additional information may be found online in the Supporting Information section at the end of the article.

mice. In conclusion, TEG011 is well tolerated without harming HLA-A*24:02^{+} expressing healthy tissues, and TEG011 persistence seems to be crucial for long-term tumor control in vivo.

Keywords

cancer immunotherapy; efficacy; mice model; persistence; preclinical; TCR engineering; TEGs; toxicity

1 | INTRODUCTION

The presence of $\gamma\delta$T cells in various tumor types suggests their essential role in cancer immunosurveillance.[1–3] However, the biological mechanism and ligand recognitions for $\gamma\delta$T cell activation remain to be elucidated. The most prevalent $\gamma\delta$T cell subset found in human peripheral blood expresses a $\gamma 9\delta 2$TCR. $\gamma 9\delta 2$T cells mediate antitumor reactivity against hematologic and solid malignancies by sensing early metabolic changes through joint spatial and conformational changes in CD277 partially mediated by RhoB (CD277J).[4–7] On the other hand, very little is known about the antitumor properties of $\gamma\delta$T cells harboring $\gamma\delta$TCRs from other subfamilies (non-$\gamma 9\delta 2$ $\gamma\delta$T cells). One of the non-$\gamma 9\delta 2$ $\gamma\delta$T cell subset, V$\delta 1^{+}$ T cells, which mainly reside in tissues, are known to recognize stress-induced ligands, including MHC-associated proteins MICA and MICB, CMV-associated glycoprotein UL16, and foreign lipid antigens presented on CD1c and CD1d in classical HLA-like manner, which are often up-regulated on stressed or malignant cells.[8–12] Several studies have also shown the cytotoxic activity of V$\delta 1^{+}$ T cells against leukemia and solid tumors,[13–15] thereby revealing their therapeutic potential.

Despite the therapeutic potential of $\gamma\delta$T cells, their successful clinical implementation remains challenging. For example, adoptive transfer of in vitro expanded $\gamma 9\delta 2$T cell failed to show clinical responses to date[3,16] whereas adoptive transfer of ex vivo expanded non-$\gamma 9\delta 2$T cells[17] remain to be tested in the clinic. Major remaining hurdles encompass diversity in function and receptor expression as well as differences in products when generated from different donors (for review see Sebestyen et al.[3]). To partially overcome these obstacles, we introduced the concept of TEGs: $\alpha\beta$T cells engineered to express a defined $\gamma\delta$TCR. TEGs allow the production of $\alpha\beta$T cells transduced with highly tumor-reactive $\gamma\delta$TCR from both V$\delta 2^{+}$[18–20] and V$\delta 2^{-}$[21–23] subsets and thereby engineering strong tumor reactivity against a broad panel of malignancies. Within this context, we previously identified an allo-HLA-restricted and CD8α-dependent Vγ5Vδ1TCR. When this particular receptor was utilized for the TEG concept (later referred as TEG011) selective reactivity toward HLA-A*24:02 expressing tumor cells, but not healthy tissues was observed.[24] However, safety studies have been so far very limited and also in vivo persistence and expansion profiles have not been assessed but are crucial before first-in-men studies. To further enrich the preclinical safety and efficacy studies needed for regulatory approval, we describe now a more detailed safety profile as well as pharmacokinetics of TEG011 after infusion in nontumor bearing and tumor-bearing humanized HLA-A*24:02 transgenic NSG (NSG-A24:02) mice and their association with tumor control.

2 | MATERIALS AND METHODS

2.1 | Retroviral transductions of T cells

TEGs were produced as previously described.[5] Briefly, Phoenix-Ampho cells were transfected with *gag-pol* (pHIT60), *env* (pCOLT-GALV), and pMP71 retroviral constructs containing both $\gamma\delta$TCR chains separated by a ribosomal skipping T2A sequence, using FugeneHD reagent (Promega, Leiden, The Netherlands). Human PBMCs from a healthy donor were pre-activated with 30 ng/mL anti-CD3 (Orthoclone OKT3; Janssen-Cilag, Breda, The Netherlands) and 50 IU/mL IL-2 (Proleukin, Novartis, Arnhem, The Netherlands) and subsequently transduced twice with viral supernatant within 48 h in the presence of 50 IU/mL IL-2 and 6 μg/mL polybrene (Sigma-Aldrich, Zwijndrecht, The Netherlands). TCR-transduced T cells were expanded by stimulation with anti-CD3/CD28 Dynabeads (500,000 beads/10^6 cells; Thermo Fisher Scientific, Breda, The Netherlands) and 50 IU/mL IL-2. Thereafter, TCR-transduced T cells were depleted of the nonengineered T cells.

2.2 | Depletion of nonengineered T cells

Depletion of nonengineered T cells was performed as previously described.[19] Briefly, TCR-transduced T cells were incubated with a biotin-labeled anti-$\alpha\beta$TCR antibody (clone BW242/412; Miltenyi Biotec, Leiden, The Netherlands) and incubated with an anti-biotin antibody coupled to magnetic beads (anti-biotin MicroBeads; Miltenyi Biotec). Thereafter, the cell suspension was loaded onto an LD column and $\alpha\beta$TCR$^+$ T cells were depleted by MACS cell separation per the manufacturer's protocol (Miltenyi Biotec). After depletion, TEGs were expanded biweekly with 1μg/mL PHA-L (Sigma-Aldrich), 50U/mL IL-2, 5 ng/mL IL-15 (Miltenyi Biotec, Leiden, The Netherlands), and irradiated allogeneic PBMCs, Daudi, and LCL-TM cells. IL-2 and IL-15 was added twice a week as reported also for the T cell rapid expansion protocol (REP).[5]

2.3 | Animal model

The NOD.Cg-*Prkdc*^{scid} *Il2rg*^{tm1Wjl} Tg(HLA-A24)3Dvs/Sz (NSG-A24:02) mice[25] were bred and housed in the breeding unit of the Central Animal Facility of Utrecht University as previously reported.[24] Experiments were conducted under institutional guidelines after permission from the local Ethical Committee and in accordance with the current Dutch laws on Animal Experimentation. Mice were housed in sterile conditions using an individually ventilated cage (IVC) system and fed with sterile food and water. Irradiated mice were given sterile water with antibiotic ciproxin for the duration of the experiment. Mice were randomized with equal distribution by sex and divided into 5 mice/group (for nontumor-bearing model) or 9–10 mice/group (for tumor-bearing model). For the nontumor-bearing mouse model, adult NSG-A24:02 mice (8–11 wk old) received sublethal total body irradiation (1.75 Gy) on day 1 followed by two injections of 1×10^7 TEG011 or TEG expressing a nonfunctional $\gamma\delta$TCR (TEG-LM1)[6] on days 1 and 6. Mice were monitored at least twice a week for weight loss and graft-versus-host disease (GvHD) symptoms (scoring parameter included hunched appearance, activity, fur texture, skin integrity, and diarrhea). The GvHD scoring system is listed in Supporting Information Table S1. Humane endpoint (HEP) was reached when mice experienced a 20% weight loss from the initial weight

(measured on day 1) and in the case of GvHD score 2 was reached for an individual GvHD parameter or a total GvHD score of 4. For the tumor-bearing mouse model, adult NSG-A24:02 mice (8–11 wk old) received sublethal total body irradiation (1.75 Gy) on day 1 followed by intravenous injection of 1×10^5 K562 HLA-A*24:02 luciferase tumor cells on day 0, and received 2 injections of TEG011 and TEG-LM1 mock on days 1 and 6 as previously reported.[24] All mice received 0.6×10^6 IU of IL-2 (Proleukin; Novartis) in 100 μl incomplete Freund's adjuvant (IFA) subcutaneously together with the first TEGs injection and every 3 weeks until the end of the experiment. Mice were monitored at least twice a week for weight loss and clinical appearance scoring (scoring parameter included hunched appearance, activity, fur texture, and piloerection). The clinical appearance scoring system is listed in Supporting Information Table S2. HEP was reached when mice experienced a 20% weight loss from the initial weight (measured on day 1), showed symptoms of disease (sign of paralysis, weakness, and reduced motility), extramedullary tumor masses (if any) reached 2 cm^3 in volume and in the case of clinical appearance score 2 was reached for an individual parameter or a total score of 4.

2.4 | Flow cytometry analysis

The following antibodies were used for flow cytometry analysis: huCD45-PB (clone HI30; Sony Biotechnology, Surrey, United Kingdom), mCD45-APC (clone 30-F11, Sony Biotechnology), $\alpha\beta$TCR-FITC (clone IP26; Biolegend, London, United Kingdom), pan-$\gamma\delta$TCR-PE (clone IMMU510; Beckman Coulter, Woerden, The Netherlands), CD8-PerCPCy5.5 (clone RPA-T8, Biolegend), CD4-PeCy7 (clone TPA-R4, Biolegend), and Vδ1-FITC (clone TS8.2, Thermo Fisher Scientific, Breda, The Netherlands). To exclude nonviable cells from the analysis, Fixable Viability Dye eFluor506 was used (eBioscience, Thermo Fisher Scientific). All samples were analyzed on a BD LSRFortessa using FACS-Diva Software (BD Biosciences).

2.5 | Assessment for TEGs persistence

Mouse peripheral blood samples were obtained via cheek vein (maximum 50–80 μl/mouse) once a week. Human cells in peripheral blood were quantified using Flow-count Fluorospheres (Beckman Coulter). Red blood cell lysis was performed for blood samples using 1× RBC lysis buffer (Biolegend) before cell staining. Blood samples were stained with a mixture of antibody panels as listed above. The persistence of TEG cells was measured in peripheral blood by quantifying for absolute cell number by flow cytometry using specific markers huCD45$^+$ $\gamma\delta$TCR$^+$CD8$^+$.

2.6 | Preparation of single cell suspensions

At the end of the study, extramedullary tumor (if any) sections were isolated and processed into single cell suspensions as previously described.[26] A small section of the extramedullary tumor masses was minced and passed through a 70 μm cell strainer (BD Biosciences); cells were washed in PBS and resuspended in RPMI 1640 Medium, GlutaMAX™ Supplement, HEPES (Thermo Fisher Scientific). A total of 10^6 cells were stained and analyzed for tumor burden (determined by GFP$^+$ cells) by flow cytometry analysis (BD LSRFortessa). Human cells were measured by quantifying absolute cell numbers from a total of 10^6 cells using Flow-count Fluorospheres (Beckman Coulter).

2.7 | Histology staining and analysis

Histopathologic evaluation was performed by H&E staining for the following mouse tissues: liver, spleen, small (duodenum, jejunum, ileum) intestine, bone marrow, and extramedullary tumor masses. When present, histologic lesions in major organs were semi-quantitatively evaluated based on the following criteria: (i) white pulp atrophy; (ii) extramedullary hematopoiesis (EMH) and cell type (including blasts, erythroid precursors, band cells, and megakaryocytes); and (iii) the presence of pigment and apoptotic cells. Bone marrows were evaluated based on the following criteria: (i) cellularity (percentage of hematopoietic cells relative to marrow fat); (ii) ratio of the myeloid and erythroid precursors (M/E ratio); and (iii) the presence of megakaryocytes. The grading system was used as follows: 0 = absent; 1 = minimal; 2 = mild; 3 = moderate; and 4 = marked.

Extramedullary tumor masses were evaluated based on the following histologic features: number of mitotic figures and apoptotic cells (express as a range per high-power fields (HPFs), calculated in the same, randomly selected 5 HPFs, 40×); extension of the necrotic tumor tissue and associated inflammation were graded from 0 to 4 (0: no lesions; 1: minimal; 2: mild; 3: moderate; and 4: severe).

Images were taken using an Olympus BX45 microscope with the Olympus DP25 camera and analyzed using DP2-BSW (version.2.2) software.

2.8 | Double immunofluorescence (IF) staining

Formalin-fixed extramedullary tumor masses were embedded in paraffin and cut into 4 μm sections. After deparaffinization and dehydration, slides were pretreated with 10 mM citrate buffer pH 6.0 for 15 min, followed by cooling at room temperature for 30 min. Immunofluorescent staining was done using anti-human Anti-Nuclei Antibody (dilution 1:100; clone 3E1.3, Merck Millipore BV, North-Holland, The Netherlands) and anti-human CD3 polyclonal antibody (dilution 1:250; Agilent Technologies, Amstelveen, The Netherlands). Slides were mounted in VECTASHIELD Antifade Mounting Medium with DAPI (Vector Laboratories, Peterborough, United Kingdom). Images were taken using a Leica LMD7 fluorescence microscope and analyzed using LAS X (Leica Application Suite X) imaging software.

2.9 | Statistical analyses

Data were analyzed using GraphPad Prism (GraphPad Software, Inc., La Jolla, CA, USA) and represented as mean ± SD or SEM with $*P < 0.05$ and $**P < 0.01$. Differences between groups were assessed using a 2-way ANOVA with repeated measures, a mixed-effects model with repeated measures, a nonparametric Mann-Whitney t-test, or Kruskal-Wallis test where indicated.

3 | RESULTS

3.1 | TEG011 do not exhibit off-target toxicity in major organs of nontumor bearing NSG-A24:02 mice

The introduction of a novel allo-HLA-restricted and CD8α-dependent Vγ5Vδ1TCR in the concept of TEGs ($\alpha\beta$T cells Engineered to express a defined $\gamma\alpha$TCR),[6,19] hereby known as TEG011, has shown its efficacy against HLA-A*24:02 expressing malignant cells in vitro as well as in vivo.[24] However, to date, in vivo efficacy and toxicity studies are limited but essential for a first-in-men study with TEG011. Therefore, we extended our in vivo analysis to assess in more detail the safety profile of TEG011 in a separate set of nontumor bearing NSG mice, which express human HLA-A*24:02 (NSG-A24:02). Nontumor bearing NSG-A24:02 mice received either two infusions of TEG011 or mock control TEG-LM1 cells. $\gamma\delta$TCR expression for both TEG011 and TEG-LM1 mock was comparable (Supporting Information Fig. S1A) and most of the transduced $\alpha\beta$T cells expressed V$\delta1^+$ TCR for TEG011 (Supporting Information Fig. S1B). Mice were subsequently monitored for T cell persistence and any possible manifestation of GvHD and any other signs of toxicity (experimental outline Fig. 1A). GvHD-like symptoms were monitored twice weekly for all mice using a scoring system based on hunching posture, activity, fur texture, skin integrity, and diarrhea (See Supporting Information Table S1 for GvHD scoring system) ranging from 0 (normal behavior and posture), 1 (slight decreased in fitness), and 2 (moderate decreased in fitness). Score 2 of an individual parameter or an overall score of 4 was defined as HEP and mice were sacrificed. All mice did neither experience weight loss, nor any abnormality observed in relation to GvHD symptoms during the entire study duration of 72 d (Fig. 2A). In addition, all mice did not exhibit any observable discomfort and survived throughout the entire study duration.[24] Persistence of TEGs was assessed by measuring viable huCD45$^+$ $\gamma\delta$TCR$^+$CD8$^+$ in mouse peripheral blood by flow cytometry (Supporting Information Fig. S2A). In nontumor-bearing mice, T cells persisted in peripheral blood up to 48 d after infusion and had although not significant a second peak of expansion after administration of IL-2, which was more pronounced in TEG011-treated mice (Fig. 3A). To evaluate in more detail possible off-target toxicity of TEG011 against human HLA-A*24:02 expressing healthy tissues, we collected bone marrow, liver, intestine, and spleen from both treatment groups of nontumor-bearing mice at the end of the study period (day 72) for further histopathology analysis (Fig. 2B). No differences were observed in terms of bone marrow cellularity (percentage of hematopoietic cells relative to marrow fat) nor in the ratio of the myeloid and erythroid precursors (M/E ratio) for both treatment group (Supporting Information Table S3). Furthermore, no abnormal histologic lesions were observed in liver (Fig. 2C) and intestine (Fig. 2D) of all mice in the study. We observed slightly increased EMH in the spleen of TEG011-treated female mice when compared to TEG-LM1 mock-treated mice (Fig. 2E), which was determined by a higher number of erythrocyte precursors and megakaryocytes. On the other hand, a minimal decrease of EMH was observed in the spleen of the TEG011-treated male group compared to mock-treated mice (Supporting Information Table S3). Importantly, all spleen samples from both TEG011 and TEG-LM1 mock groups showed a comparable population of cells, including normal blasts, band cells, erythrocyte precursors, and megakaryocytes. Hence, these observations on spleen were deemed minimal and not associated with an evident increase of histologic toxicity of

TEG011. In conclusion, our data show no relevant GvHD manifestation in all mice and no histologic signs of toxicity in the major organs of all healthy tissues upon TEG011 treatment. Thus, we conclude that TEG011 does not associate with off-target toxicity in an HLA–A*24:02 environment.

3.2 | In vivo dynamic of TEG011 in tumor-bearing mice

Clinical data for anti-CD19 chimeric antigen receptor T cell (CART) therapy highlight the correlation of antitumor effects with their in vivo persistence.[27–29] To assess whether persistence of TEG011, which carries a CD8α-dependent Vγ5Vδ1TCR,[24] is also key in long-term tumor control, we studied in more detail $CD8^+$ TEG persistence in tumor-bearing NSG-A24:02 mice injected with K562 HLA-A*24:02 luciferase tumor cells and subsequently treated with either TEG011 or TEG-LM1 mock cells (experimental outline Fig. 1B). Thereafter, we measured viable $huCD45^+\gamma\delta TCR^+CD8^+$ in mouse peripheral blood by flow cytometry (Supporting Information Fig. S2B). Whereas nonfunctional TEG-LM1 cells diminished in all tumor-bearing control mice 29 d after infusion (Fig. 3B), TEG011 cells expanded and remained detectable in peripheral blood up to 64 d. However, only 44% of TEG011-treated mice (4/9) showed significant long-term persistence of T cells until the end of the study period, whereas the remaining 56% of the mice (5/9) did not show long-term persistence. Therefore, we subsequently defined TEG011-treated mice into two subgroup: “persisters” and “nonpersisters,” respectively (Fig. 3C). TEG011 “persisters” showed significantly higher TEG cell counts on day 22 until day 37 upon expansion compared to “nonpersisters,” where TEG cells were no longer detectable after day 48 and did not recover even after IL-2 injection on day 50. Given the fluctuating persistence profile of TEG011, we analyzed further the difference between TEG011 “persisters” and “nonpersisters” by calculating area under curve (AUC) of absolute cell counts TEG011 for both “persisters” and “nonpersisters” subgroup and also confirmed significant difference in T cell persistence (Fig. 3C, D).

3.3 | TEG011 persistence and its association with tumor control

Next, we assessed whether TEG011 persistence was associated with overall tumor control and analyzed tumor burden over time measured by bioluminescence imaging (BLI) in the tumor-bearing mice injected with K562 HLA-A*24:02 luciferase tumor cells. In line with our hypothesis that the immune effector persistence is key to achieve long-term tumor control, the TEG011 “persisters” associated with a better tumor control as compared to TEG-LM1 mock group, as well as a trend of lower tumor burden in comparison to TEG011 “nonpersisters” subgroup (Fig. 3E). Approximately 40% of mock-treated mice (4/10) and 40% TEG011 “nonpersisters” mice(2/5) developed extramedullary tumor masses, whereas interestingly, none of the TEG011 “persisters” mice developed any extramedullary tumor masses. Tumor burden was comparable between extramedullary tumor masses isolated from TEG011 “nonpersisters” and TEG-LM1 mock-treated mice and no tumor infiltrating $CD8^+$ TEGs could be observed in all isolated tumor masses (Fig. 3F).

To measure possible discomfort due to tumor growth, all mice were monitored for weight loss and a scoring system based hunching posture, activity, fur texture, and piloerection (See Supporting Information Table S2 for clinical appearance scoring system) ranging from 0

(normal behavior and posture), 1 (slight decreased in fitness), and 2 (moderate decreased in fitness). Similar to GvHD scoring system for nontumor-bearing mice, score 2 of an individual parameter or an overall score of 4 was defined as HEP and mice were sacrificed. Whereas TEG011 treatment significantly decreased tumor progression, TEG-LM1 treated mice experienced diminished fitness and significant weight loss over time (Fig. 4A). Extramedullary tumor masses were analyzed in further detail and histologically characterized by undifferentiated tumor cells of human origin, with a solid and invasive growth pattern (Fig. 4B, C), consistent with a myeloid sarcoma development in line with previous reports.[30,31] We also performed IF staining to detect any presence of human T cells within the inflammatory infiltrate associated with the multiple tumor masses observed in the xenograft mouse models. However, whereas we confirmed that tumor cells are of human origin, no human T cells were observed in all evaluated samples, as scattered positive $CD3^+$ T cells observed within the multiple tumor masses were all negative for the human nuclear antigen (Fig. 4D). Thus, no TEGs could be observed by immunohistochemistry in extramedullary tumor masses as also confirmed by flow cytometry analysis (Fig. 3F). Overall, our data indicate that TEG011 persistence associates with a reduced chance for developing extramedullary tumor masses in vivo without harming healthy compartments.

4 | DISCUSSION

TEG011 has been reported to target HLA-A*24:02 expressing hematologic tumors without harming healthy tissues.[24] Within this study, we now extend previous in vivo analyses followed by pathological studies to further assess the efficacy-toxicity balance of TEG011 prior to clinical testing. Major findings of our study are that TEG011 treatment does not associate with any discomfort nor histopathologic evidence of toxicity in an HLA-A*24:02 background. In addition, we report on an association between TEG011 persistence and lack of extramedullary tumor growth.

Toxicity studies of compounds targeting metabolic changes remain a major challenge as such changes cannot be readily studied in detail in all organs.[3] Therefore, we proposed efficacy-toxicity models for TEGs targeting joint spatial and conformational changes in CD277 (later referred as CD277J)[3] through a $\gamma 9\delta 2$TCR (TEG001) by co-incubating TEG001 with healthy and diseased tissues in an artificial 3D bone marrow niche[32] or in a mouse model where either healthy cord blood-derived $CD34^+$ progenitor or primary leukemia cells were engrafted.[26] These models partially overcome the absence of the natural ligand CD277J in mice[3,7,33] and allowed the initiation of a first-in-men study (NTR6541).[18,19,34] With TEG011, we could utilize transgenic mice expressing human HLA-A*24:02,[25] allowing thereby more extensive toxicity studies of TEG011 in different tissues as compared to TEG001.[26,32] Although we did not investigate all organs, and despite the fact that TEG011 did not persist until day 72 in the peripheral blood of all mice, we provide strong evidence that TEG011 does not induce toxicity against human HLA-A*24:02 expressing nontumor healthy tissues. This is also supported by our observation that tumor control in mice did not associate with any signs of toxicity against healthy tissues.

Considering the natural properties of T cells to proliferate and migrate in tissues, T cell expansion and persistence are commonly used to determine the pharmacokinetics properties

of cell-based therapy.[35] Our models also allowed us to investigate TEG011 kinetics in tumor-bearing mice in more detail. TEG persistence until the end of the study period was only observed in tumor-bearing mice treated with TEG011 but not in TEG-LM1 cells, suggesting that antigen presence and cognate recognition through the TCR are key for long-term persistence of TEG011 in this model. Higher T cell exposure observed between days 22 and 36 after TEG infusion correlated with superior tumor control of TEG011 ("persisters"). These data align with a recent study that showed complete response in leukemia patients who receive CART therapy when high T cell exposure has been observed in the first 48 d of infusion.[36]

However, TEG011 long-term persistence was only observed in 44% of tumor-bearing mice. Within the limitation of our model, we could not identify the exact factor(s) that determine the difference between TEG011 "persisters" and "nonpersisters." Most likely this is the consequence of a stochastically driven intrinsic T cell fitness and composition of the infused product. The presence of memory (stem) T cells has been reported to correlate with long-term persistence[37,38] and complete response in patients receiving adoptive transfers of CART or antigen-specific T cells.[37,38]

Furthermore, in nontumor-bearing mice some advantage of the TEG011 product has been observed when compared to T cell bearing the nonfunctional receptor, though no long-term persistence has been observed. This might be the consequence of some residual TCR signal via HLA-A*24:02, which is sufficient to maintain some homeostatic proliferation but does not induce toxicity in healthy tissues. In particular, after administration of IL-2 T cell survival of cognate T cells in tumor-bearing mice has been prolonged suggesting that additional help through, for example, $CD4^+$ engineered T cells could further improve potency of TEG011. Indeed, the presence of antigen-specific TCR-engineered $CD4^+$ T cells synergistically enhances persistence and long-term tumor control when infused together with antigen-specific TCR-engineered $CD8^+$ T cells.[39] Similarly, in vivo persistence of $CD4^+$ CART cells provides helper signal, which then increases $CD8^+$ CART cell persistence.[40]

As TEG011 is CD8α dependent and consequently in the current design lacking support by antigen-specific $CD4^+$ T cells,[22,24] equipping engineered TEG011 with CD8$\alpha\alpha$ could be a strategy to further enhance T cell persistence and long-term tumor control. However, the precise molecular interaction between CD8$\alpha\alpha$ and its specific ligand in our context remains elusive. Possible ligands are the classical MHC-I molecule HLA-A*24:02 itself or alternative candidates such as the nonclassical MHC molecule HLA-G[41,42] and CEACAM5.[43]

Overall, we demonstrate that TEG011 does not show signs of off-target toxicity in more detailed toxicity studies. In addition, long-term persistence of TEG011 associated with lower tumor burden without harming healthy tissues, thereby highlights the potential of TEG011 for clinical application.

Supplementary Material

Refer to Web version on PubMed Central for supplementary material.

ACKNOWLEDGMENTS

We thank Halvard Boenig (Institute for Transfusion Medicine and Immunohematology, Goethe University, Frankfurt a. M., Germany) for providing PBMCs for feeder cells.

This work was supported by Grants ZonMW 43400003 and VIDI-ZonMW 917.11.337, KWF Grants UU 2013-6426, UU 2014-6790, UU 2015-7601, and Gadeta (to J.K.); Grant UU 2017-11393 (to Z.S. and J.K.); Marie Curie Grant 749010 (to D.B.); and the National Institutes of Health (NIH) grants CA34196 and OD026440 (to L.D.S.).

Abbreviation:

AUC	Area under curve
BLI	Bioluminescence imaging
CART	Chimeric antigen receptor T cell
EMH	Extramedullary hematopoiesis
GvHD	Graft-versus-host disease
HEP	Humane endpoint
HPFs	High-power fields
IF	Immunofluorescence
IFA	Incomplete Freund’s adjuvant
IVC	Individually ventilated cage
REP	Rapid expansion protocol
TEGs	$\alpha\beta$T cells engineered to express a defined $\gamma\delta$TCRs

REFERENCES

1. Dadi S, Chhangawala S, Whitlock BM, et al. Cancer immunosurveillance by tissue-resident innate lymphoid cells and innate-like T cells. Cell. 2016;164(3):365–377. [PubMed: 26806130]
2. Gentles AJ, Newman AM, Liu CL, et al. The prognostic landscape of genes and infiltrating immune cells across human cancers. Nat Med. 2015;21(8):938–945. [PubMed: 26193342]
3. Sebestyen Z, Prinz I, Dechanet-Merville J, Silva-Santos B, Kuball J. Translating gammadelta (γδ) T cells and their receptors into cancer cell therapies. Nat Rev Drug Discov. 2019.
4. Kabelitz D, Wesch D, He W. Perspectives of γδ T cells in tumor immunology. Cancer Res. 2007;67(1):5–8. [PubMed: 17210676]
5. Marcu-Malina V, Heijhuurs S, van Buuren M, et al. Redirecting αβT cells against cancer cells by transfer of a broadly tumor-reactive γδT-cell receptor. Blood. 2011;118(1):50–59. [PubMed: 21566093]
6. Grunder C, van Dorp S, Hol S, et al. γ9 and δ2CDR3 domains regulate functional avidity of T cells harboring γ9δ2TCRs. Blood. 2012;120(26): 5153–5162. [PubMed: 23018643]
7. Sebestyen Z, Scheper W, Vyborova A, et al. RhoB mediates phosphor-antigen recognition by Vγ9Vδ2 T cell receptor. Cell Rep. 2016;15(9): 1973–1985. [PubMed: 27210746]
8. Groh V, Rhinehart R, Secrist H, Bauer S, Grabstein KH, Spies T. Broad tumor-associated expression and recognition by tumor-derived γδT cells of MICA and MICB. Proc Natl Acad Sci USA. 1999;96(12): 6879–6884. [PubMed: 10359807]

9. Catellani S, Poggi A, Bruzzone A, et al. Expansion of Vδ1 T lymphocytes producing IL-4 in low-grade non-Hodgkin lymphomas expressing UL-16-binding proteins. Blood. 2007;109(5):2078–2085. [PubMed: 16973957]
10. Poggi A, Venturino C, Catellani S, et al. V 1 T lymphocytes from B-CLL patients recognize ULBP3 expressed on leukemic B cells and up-regulated by trans-retinoic acid. Cancer Res. 2004;64(24):9172–9179. [PubMed: 15604289]
11. Luoma AM, Castro CD, Mayassi T, et al. Crystal structure of Vδ1 T cell receptor in complex with CD1d-sulfatide shows MHC-like recognition of a self-lipid by human γδT cells. Immunity. 2013;39(6):1032–1042. [PubMed: 24239091]
12. Zhao J, Huang J, Chen H, Cui L, He W. Vδ1 T cell receptor binds specifically to MHC I chain related A: molecular and biochemical evidences. Biochem Biophys Res Commun. 2006;339(1):232–240. [PubMed: 16297874]
13. Schilbach K, Frommer K, Meier S, Handgretinger R, Eyrich M. Immune response of human propagated γδ-T-cells to neuroblastoma recommend the $V\delta1^+$ subset for γδ-T-cell-based immunotherapy. J Immunother. 2008;31(9):896–905. [PubMed: 18832998]
14. Maeurer MJ, Martin D, Walter W, et al. Human intestinal $V\delta1^+$ lymphocytes recognize tumor cells of epithelial origin. J Exp Med. 1996;183(4):1681–1696. [PubMed: 8666926]
15. Devaud C, Rousseau B, Netzer S, et al. Anti-metastatic potential of human $V\delta1^+$ γδT cells in an orthotopic mouse xenograft model of colon carcinoma. Cancer Immunol Immunother. 2013;62(7):1199–1210. [PubMed: 23619975]
16. Deniger DC, Moyes JS, Cooper LJ. Clinical applications of γδT cells with multivalent immunity. Front Immunol. 2014;5:636. [PubMed: 25566249]
17. Siegers GM. Cytotoxic and regulatory properties of circulating $V\gamma\delta1^+$ γδT cells: a new player on the cell therapy field?. Mol Ther. 2014;22(8):1416–1422. [PubMed: 24895997]
18. Straetemans T, Kierkels GJJ, Doorn R, et al. GMP-grade manufacturing of T cells engineered to express a defined γδTCR. Front Immunol. 2018;9:1062. [PubMed: 29899740]
19. Straetemans T, Grunder C, Heijhuurs S, et al. Untouched GMP-ready purified engineered immune cells to treat cancer. Clin Cancer Res. 2015;21(17):3957–3968. [PubMed: 25991821]
20. Straetemans T, Janssen A, Jansen K, et al. TEG001 insert integrity from vector producer cells until medicinal product. Mol Ther. 2019.
21. Scheper W, Sebestyen Z, Kuball J. Cancer immunotherapy using γδT cells: dealing with diversity. Front Immunol. 2014;5:601. [PubMed: 25477886]
22. Scheper W, van Dorp S, Kersting S, et al. γδT cells elicited by CMV reactivation after allo-SCT cross-recognize CMV and leukemia. Leukemia. 2013;27(6):1328–1338. [PubMed: 23277330]
23. Scheper W, Grunder C, Straetemans T, Sebestyen Z, Kuball J. Hunting for clinical translation with innate-like immune cells and their receptors. Leukemia. 2014;28(6):1181–1190. [PubMed: 24345790]
24. Kierkels GJJ, Scheper W, Meringa AD, et al. Identification of a tumor-specific allo-HLA-restricted γδTCR. Blood Adv. 2019;3(19): 2870–2882. [PubMed: 31585951]
25. Najima Y, Tomizawa-Murasawa M, Saito Y, et al. Induction of WT1-specific human $CD8^+$ T cells from human HSCs in HLA class I Tg NOD/SCID/IL2rgKO mice. Blood. 2016;127(6): 722–734. [PubMed: 26702062]
26. Johanna I, Straetemans T, Heijhuurs S, et al. Evaluating in vivo efficacy - toxicity profile of TEG001 in humanized mice xenografts against primary human AML disease and healthy hematopoietic cells. J Immunother Cancer. 2019;7(1):69. [PubMed: 30871629]
27. Porter DL, Hwang WT, Frey NV, et al. Chimeric antigen receptor T cells persist and induce sustained remissions in relapsed refractory chronic lymphocytic leukemia. Sci Transl Med. 2015;7(303):303ra139.
28. Brentjens RJ, Riviere I, Park JH, et al. Safety and persistence of adoptively transferred autologous CD19-targeted T cells in patients with relapsed or chemotherapy refractory B-cell leukemias. Blood. 2011;118(18):4817–4828. [PubMed: 21849486]
29. Kochenderfer JN, Dudley ME, Feldman SA, et al. B-cell depletion and remissions of malignancy along with cytokine-associated toxicity in a clinical trial of anti-CD19 chimeric-antigen-receptor-transduced T cells. Blood. 2012;119(12):2709–2720. [PubMed: 22160384]

30. Lozzio BB, Lozzi CB, Machado E. Human myelogenous (Ph+) leukemia cell line: transplantation into athymic mice. J Natl Cancer Inst. 1976;56(3):627–629. [PubMed: 1062625]
31. Caretto P, Forni M, d'Orazi G, et al. Xenotransplantation in immuno-suppressed nude mice of human solid tumors and acute leukemias directly from patients or in vitro cell lines. Ric Clin Lab. 1989;19(3): 231–243. [PubMed: 2595194]
32. Braham MVJ, Minnema MC, Aarts T, et al. Cellular immunotherapy on primary multiple myeloma expanded in a 3D bone marrow niche model. Oncoimmunology. 2018;7(6):e1434465.
33. Harly C, Guillaume Y, Nedellec S, et al. Key implication of CD277/butyrophilin-3 (BTN3A) in cellular stress sensing by a major human γδT-cell subset. Blood. 2012;120(11):2269–2279. [PubMed: 22767497]
34. Kierkels GJ, Straetemans T, de Witte MA, Kuball J. The next step toward GMP-grade production of engineered immune cells. Oncoimmunology. 2016;5(2):e1076608.
35. Kakkanaiah VN, Lang KR, Bennett PK. Flow cytometry in cell-based pharmacokinetics or cellular kinetics in adoptive cell therapy. Bioanalysis. 2018;10(18):1457–1459. [PubMed: 30215270]
36. Mueller KT, Maude SL, Porter DL, et al. Cellular kinetics of CTL019 in relapsed/refractory B-cell acute lymphoblastic leukemia and chronic lymphocytic leukemia. Blood. 2017;130(21):2317–2325. [PubMed: 28935694]
37. Xu Y, Zhang M, Ramos CA, et al. Closely related T-memory stem cells correlate with in vivo expansion of CAR.CD19-T cells and are preserved by IL-7 and IL-15. Blood. 2014;123(24): 3750–3759. [PubMed: 24782509]
38. Louis CU, Savoldo B, Dotti G, et al. Antitumor activity and long-term fate of chimeric antigen receptor-positive T cells in patients with neuroblastoma. Blood. 2011;118(23):6050–6056. [PubMed: 21984804]
39. Morris EC, Tsallios A, Bendle GM, Xue SA, Stauss HJ. A critical role of T cell antigen receptor-transduced MHC class I-restricted helper T cells in tumor protection. Proc Natl Acad Sci USA. 2005;102(22):7934–7939. [PubMed: 15908507]
40. Guedan S, Posey AD Jr, Shaw C, et al. Enhancing CAR T cell persistence through ICOS and 4–1BB costimulation. JCI Insight. 2018;3(1).
41. Sanders SK, Giblin PA, Kavathas P. Cell-cell adhesion mediated by CD8 and human histocompatibility leukocyte antigen G, a nonclassical major histocompatibility complex class 1 molecule on cytotrophoblasts. J Exp Med. 1991;174(3):737–740. [PubMed: 1908512]
42. Hofmeister V, Weiss EH. HLA-G modulates immune responses by diverse receptor interactions. Semin Cancer Biol. 2003;13(5):317–323. [PubMed: 14708711]
43. Roda G, Jianyu X, Park MS, et al. Characterizing CEACAM5 interaction with CD8α and CD1d in intestinal homeostasis. Mucosal Immunol. 2014;7(3):615–624. [PubMed: 24104458]

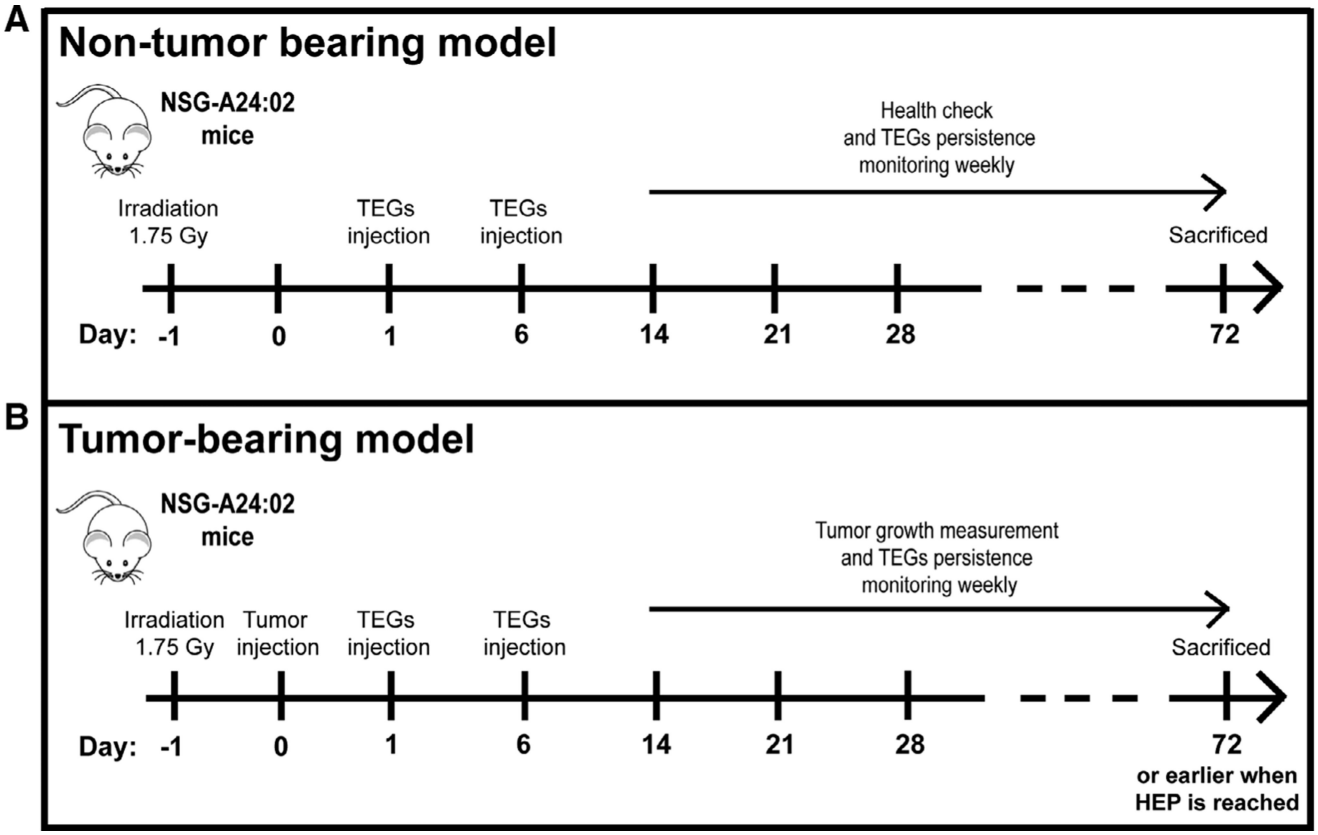

FIGURE 1. Humanized NSG-A24:02 transgenic mice models.

Schematic overview of the in vivo experiment for nontumor bearing **(A)** and K562 HLA-A*24:02 tumor-bearing mice **(B)**. Nontumor bearing NSG-A24:02 mice were irradiated at day −1 and received 2 injections of TEG011 or TEG-LM1 mock on days 1 and 6. Irradiated tumor-bearing NSG-A24:02 mice were injected with K562 HLA-A*24:02 luciferase tumor cells on day 0 followed by received 2 injections of TEG011 or TEG-LM1 mock on days 1 and 6. Mice were monitored weekly and sacrificed at day 72 or earlier when humane endpoint (HEP) is reached

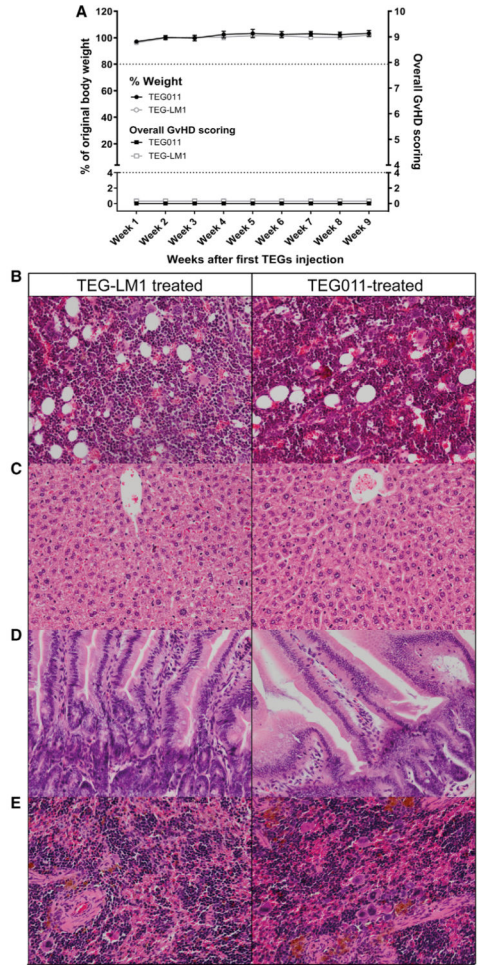

FIGURE 2. Weight loss, overall graft-versus-host disease (GvHD) scoring, and histopathology analysis of bone marrow and mouse vital organs (spleen, liver, intestine) of nontumor-bearing mice.

(A) Percentages of weight change measured weekly during study period for nontumor-bearing mice treated with TEG011 (filled black circle) and TEG-LM1 mock (open gray circle) tabulated on left *Y*-axis. A total of 20% weight loss from initial weight measured on day 1 were considered humane endpoint (HEP) and indicated by black tick line. Overall GvHD scoring was tabulated on right *Y*-axis for nontumor-bearing mice treated with TEG011 (filled black rectangle) and TEG-LM1 mock (open gray rectangle). Scoring was calculated based on following parameters: hunching, activity, fur texture, skin integrity, and diarrhea. Score range from 0 to 10 (see Supporting Information Table S1 for detail scoring system), where total overall score of 4 was considered HEP and indicated by black tick line. Score 0 depicts normal appearance for all GvHD parameters. Data represent mean ± SEM of all mice per group (n = 5 mice/group). **(B)** Representative photomicrographs H&E stained of mouse bone marrow from both TEG-LM1 mock (left panel) and TEG011-treated group (right panel). Magnification: 20×; **(C)** Representative photomicrographs for H&E stained of mouse liver for both TEG-LM1 mock (left) and TEG011-treated group (right) with apparent no histologic lesion. Magnification: 20×; **(D)** Representative pictures for H&E staining of mouse intestine for both TEG-LM1 mock (left) and TEG011-treated group (right) with

apparent no histologic lesion. Magnification: 20×; **(E)** Representative photomicrographs for H&E stained of female mouse spleen for both TEG-LM1 mock (left) and TEG011-treated group (right) with a higher number of erythrocyte precursors and megakaryocytes. Magnification: 20×; Shown are representative photomicrographs from individual mice of both TEG011 and TEG-LM1 mock group (n = 5 mice/group) with no observable differences in overall histology features between treatment groups

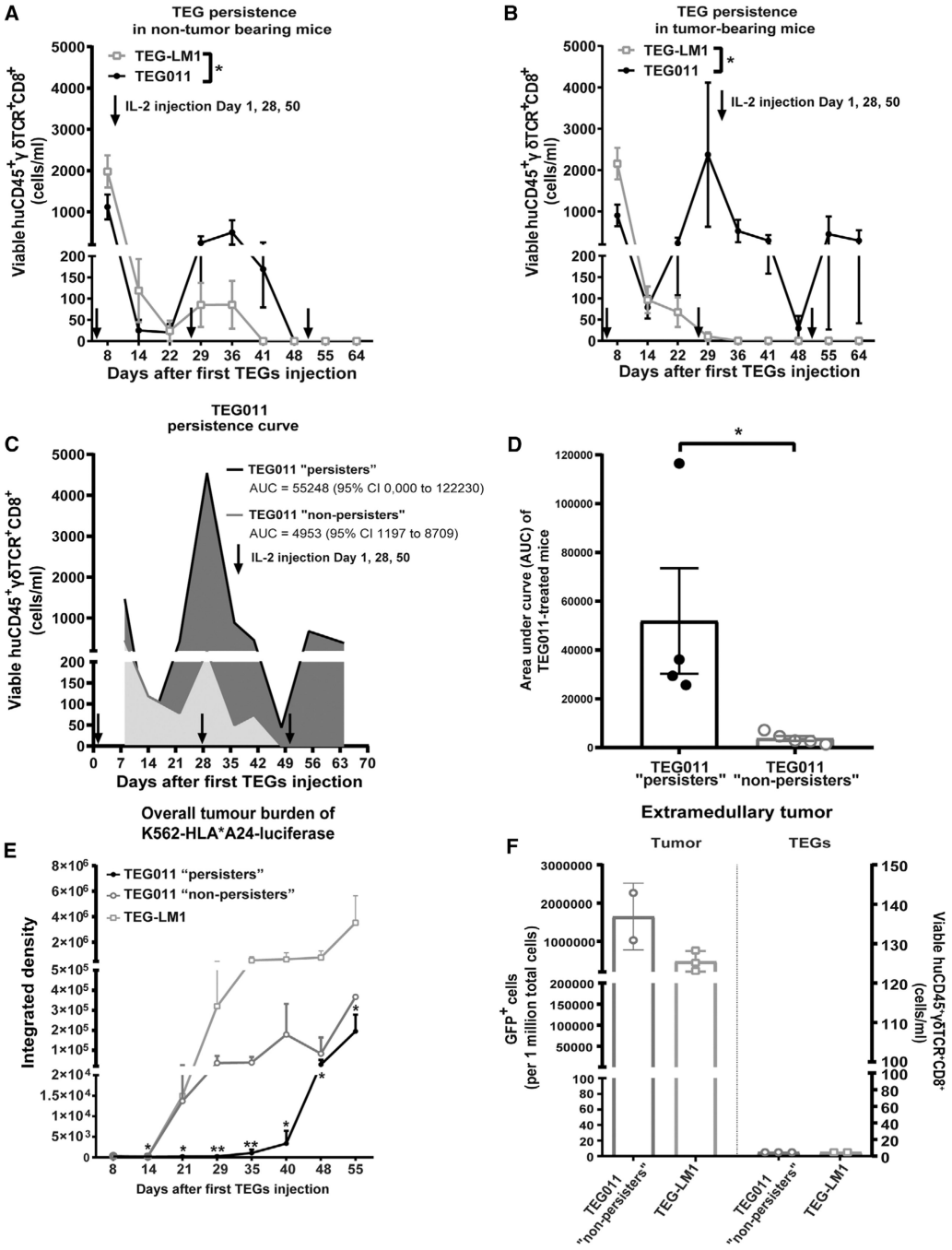

FIGURE 3. Long-term persistence of TEG011 cells in peripheral blood of tumor-bearing mice and its association with tumor burden.

(A) TEG persistence was measured in peripheral blood by quantifying for absolute cell numbers of by flow cytometry for TEG-LM1 mock (open light gray rectangle) and TEG011 (filled black circle) in nontumor-bearing mice. Data represent mean ± SEM of all mice per group ($n = 5$ mice). Statistical significances were calculated by mixed-effects model with repeated measures; *, $P < 0.05$. **(B)** TEG persistence was measured in peripheral blood by quantifying for absolute cell numbers by flow cytometry for TEG-LM1 mock (open light

gray rectangle; $n = 10$ mice) and TEG011 (filled black circle; $n = 9$ mice) in tumor-bearing mice. Data represent mean ± SEM of all mice per group. Statistical significances were calculated by mixed-effects model with repeated measures; *, $P < 0.05$. **(C)** Area under the curve (AUC) of $CD8^+$ TEG011 persistence were calculated for both TEG011 "persisters" (black line, dark gray area; 4/9 mice) and TEG011 "nonpersisters" (gray line, light gray area; 5/9 mice) up to 64 d after infusion. Data represent mean ± SEM of all mice per group. 95% Confidence Interval (95% CI) were tabulated for AUC of both subgroup. **(D)** Mean AUC of $CD8^+$ TEG011 persistence from individual mouse of both TEG011 "persisters" (filled dark gray bar; 4/9 mice) and TEG011 "nonpersisters" (filled light gray bar; 5/9 mice) groups were tabulated and shown as mean ± SEM of all mice per group. Statistical significances were calculated by nonparametric Mann-Whitney *t*-test; *, $P < 0.05$. **(E)** Tumor burden for K562 HLA*A24-luciferase was assessed in vivo by bioluminescence imaging (BLI) measuring integrated density of the entire area of mice with abdomen facing up. Data shown as mean ± SD of all mice per group (TEG011 "persisters" (filled black circle; 4/9 mice), TEG011 "nonpersisters" (open dark gray circle 5/9 mice), and TEG-LM1 mock (open light gray rectangle; $n = 10$ mice)). Statistical significances were calculated by nonparametric Mann-Whitney *t*-test in comparison to TEG-LM1 mock control; *, $P < 0.05$; **, $P < 0.01$. **(F)** Tumor burden for K562 HLA*A24-luciferase and infiltrating $CD8^+$ TEGs were assessed from isolated extramedullary tumor masses by quantifying for absolute cell number GFP^+ cells and viable $huCD45^+\gamma\delta TCR^+CD8^+$ by flow cytometry, respectively. Each symbol represents an individual mouse per treatment group that developed extramedullary tumor masses. Readouts on infiltrating T cells are set to 5 cells/mL for individual mouse in the *Y*-axis for data visualization purpose. Data represent mean ± SD of all mice per group (TEG011 "nonpersisters" (open dark gray circle; 2/5 mice) and TEG-LM1 mock (open light gray rectangle; 3/10 mice)). FACS analyses of extramedullary tumor mass from TEG-LM1 group were only obtained from 3 out of 4 mice

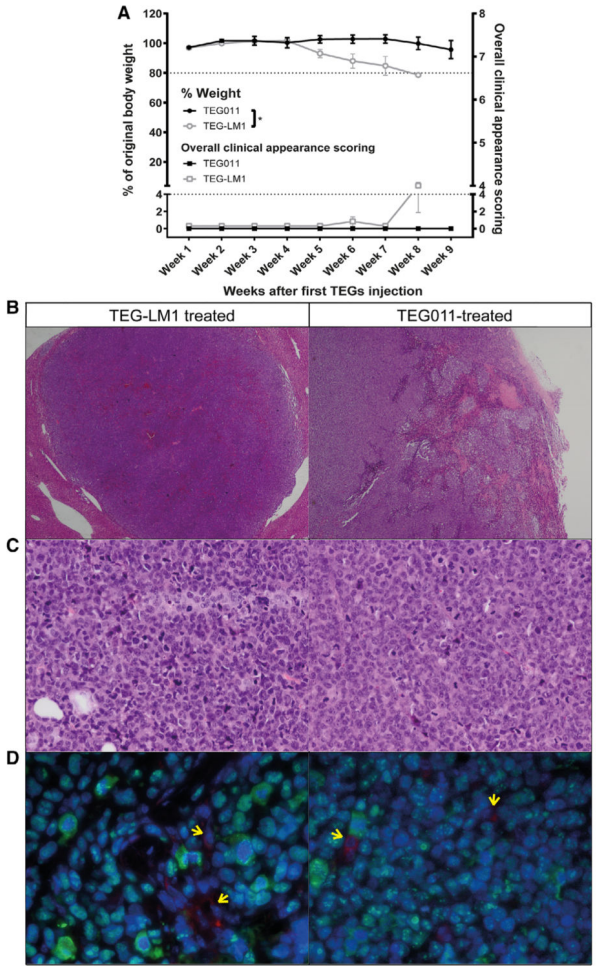

FIGURE 4. Weight loss, overall clinical appearance scoring, histopathology, and immunofluorescence (IF) staining analysis of extramedullary tumor masses.

(A) Percentages of weight loss measured weekly during study period for tumor-bearing mice treated with TEG011 (filled black circle; $n = 9$ mice) and TEG-LM1 mock (open gray circle; $n = 10$ mice) tabulated on left *Y*-axis. A total of 20% weight loss from initial weight measured on day 1 were considered humane endpoint (HEP) and indicated by black tick line. Overall clinical appearance scoring was tabulated on right *Y*-axis for tumor-bearing mice treated with TEG011 (filled black rectangle; $n = 9$ mice) and TEG-LM1 mock (open gray rectangle; $n = 10$ mice). Scoring was calculated based on following parameters: hunching, activity, fur texture, and piloerection. Score range from 0 to 8 (see Supporting Information Table S2 for detail scoring system), where total overall score of 4 were considered HEP and indicated by black tick line. Score 0 depicts normal appearance for all clinical appearance parameters. Data represent mean ± SEM of all mice per group. Statistical significances were calculated by nonparametric Mann-Whitney *t*-test; *, $P < 0.05$. **(B)** Representative photomicrographs H&E stained of extramedullary tumor masses showing multiple areas of hemorrhages and necrosis from both TEG-LM1 mock (left panel - stated as control) and TEG011-treated group (right panel). Aberrant mitotic figures were frequently observed in all samples. Magnification: 2×; **(C)** Representative photomicrographs H&E stained tissues of high mitotic rate tumor cells from both TEG-LM1 mock (left panel) and

TEG011-treated group (right panel). Magnification: 20×. No evident differences were observed comparing the extension of necrotic areas in the tumor tissue, associated inflammation, number of apoptotic cells, and mitotic figures. **(D)** Representative double IF staining of extramedullary tumor masses from both TEG-LM1 mock (left panel) and TEG011-treated group (right panel). Tumor mass of human origin (human nuclear antigen positive cells, green) with scattered CD3 positive cells (red; pointed by arrows) with DAPI (blue) staining for the nuclei. Magnification 63×. Shown are representative pictures from an individual mouse of both TEG-LM1 mock (n = 4 mice) and TEG011 (n = 2 mice)